Base Station Sleeping and Resource Allocation in Renewable Energy Powered Cellular Networks

Jie Gong, *Member, IEEE*, John S. Thompson, *Member, IEEE*, Sheng Zhou, *Member, IEEE*, Zhisheng Niu, *Fellow, IEEE*

Abstract

We consider energy-efficient wireless resource management in cellular networks where base stations (BSs) are equipped with energy harvesting devices, using statistical information for traffic intensity and renewable energy. The problem is formulated as adapting BSs' on-off states, active resource blocks (e.g. subcarriers) as well as renewable energy allocation to minimize the average grid power consumption while satisfying the users' quality of service (blocking probability) requirements. It is transformed into an unconstrained optimization problem to minimize a weighted sum of grid power consumption and blocking probability. A *two-stage dynamic programming* algorithm is proposed to solve this problem,

J. Gong, S. Zhou and Z. Niu are with Tsinghua National Laboratory for Information Science and Technology, Department of Electronic Engineering, Tsinghua University, Beijing 100084, P. R. China. Email: {gongj13, sheng.zhou, niuzhs}@tsinghua.edu.cn.

J. S. Thompson is with the Institute of Digital Communications, School of Engineering, University of Edinburgh, Edinburgh EH9 3JL, UK. Email: John.Thompson@ed.ac.uk.

This work is sponsored in part by the National Science Foundation of China (NSFC) under grant No. 61201191, the National Basic Research Program of China (973 Program: 2012CB316001), the Creative Research Groups of NSFC under grant No. 61321061, and Hitachi R&D Headquarter.

John Thompson acknowledges part funding of this work by EPSRC Grant EP/J015180/1.

by which the BSs' on-off states are optimized in the first stage, and the active BSs' resource blocks are allocated iteratively in the second stage. Compared with the optimal joint BSs' on-off states and active resource blocks allocation algorithm, the proposed algorithm greatly reduces the computational complexity, and can achieve the optimal performance when the traffic is uniformly distributed.

Index Terms

Energy harvesting, resource allocation, base station sleeping, dynamic programming.

I. Introduction

The continuously growing demands for high data rate services have made wireless communication networks one of the key sources of the world energy consumption. As a result, energy saving in wireless cellular networks is urgently required to realize green communications. One of the candidate solutions is to exploit renewable energy (e.g. solar energy, wind energy and so on) from the surrounding environment to support wireless data transmission, known as *energy harvesting* technology. Intelligently adapting the resource allocation of base stations (BSs) with energy harvesting equipment can effectively reduce the energy demand from the power grid [1], hence reducing carbon emissions. However, due to the limited availability of harvested energy as well as the uncertainty about the timing and the quantity of energy collected, it is still necessary for BSs to have access to the power grid for the quality of service (QoS) guarantee, and there is a tradeoff between QoS and the available power budget. Specifically, increasing the active wireless resource enhances the system capacity and users' service experience, but at the same time increases the probability of energy depletion, which increases the energy demand from the power grid. To reduce the energy consumption of the power grid, resource allocation should be optimized jointly considering the traffic profile, the users' QoS requirement, and the renewable energy statistics.

Resource allocation for energy harvesting systems has been extensively studied recently.

J. Yang *et. al.* analyzed the offline optimal power allocation policy in a non-fading channel [2]. In the fading channel, the optimal power allocation is interpreted as the *directional water-filling* policy [3]. The offline analysis is extended to the broadcast channel [4] [5], the multiple access channel [6] and the MIMO channel [7]. However, in practice, the energy arrival can not be known in advance due to uncertainty concerning the energy source. Consequently, the offline optimal policy is not applicable in real systems.

A practical way is to optimize the resource allocation using statistical information for harvested energy, for instance, the average arrival rate or the statistical distribution. For infinite horizon case, ref. [8] considers a cross-layer resource allocation problem to maximize the total system utility using a Markov decision process (MDP) approach [9]. The packet dropping and blocking probabilities are analyzed with different sleep and wake-up strategies in sensor/mesh networks with solar power [10]. In [11], it is shown that the wireless link is strongly influenced by the renewable energy profile, and parameter adaptation can improve the performance. Throughput optimal routing scheme is proposed in [12] for rechargeable sensor networks. The closed-form maximum stable throughput is studied and derived in cognitive radio networks [13] and cooperative networks [14], respectively. Very recently, throughput maximization scheduling has been extended to finite horizon case [15], [16]. Nevertheless, most of existing work focuses on link level analysis, while how to efficiently allocate wireless resources according to the network traffic profile and the harvested energy profile from the network point of view still remains an open problem.

Based on the measured data, the statistics of the network traffic profile [17], [18] and the harvested energy profile [19], [20] have been studied, which are shown to be predictable and hence can be assumed non-causally known. In this paper, we make use of the statistical information for traffic intensity and harvested energy to study the BS sleeping and resource allocation problem in cellular networks. We consider both deep sleep in long time scale (minutes or hours), and subframe on-off in short time scale (ms). Deep sleep allows us to greatly reduce the energy consumption utilizing the slow traffic variation, and short term sleeping in ms further exploits the energy saving potential due to the dynamics of instantaneous traffic. In the literature, BS sleeping has been studied with grid power supply only [21], [22]. In this work, a mixed power supply from both renewable energy sources and power grid is adopted. Specifically, reliable grid power guarantees that the service requirement is satisfied, while an effective renewable energy allocation policy reduces the grid power consumption. In the mixed power scenario, power allocation [23], coordinated MIMO [24] and network planning [25] has been studied. Very recent work [26] studied the resource allocation problem without considering BS sleeping. Unlike the existing work, we consider the grid power minimization problem with users' QoS constraints in a downlink cellular network by adjusting BSs' on-off states and resource block allocation. In this paper, we adopt the blocking probability as the QoS metric to exploit energy consumption behavior in terms of network traffic with data rate requirement. The preliminary results in single-cell case have been presented in [27]. This paper extensively studies the problem in a multi-cell case. The contributions are as follows:

- We formulate the problem of average grid power minimization taking into account the users' QoS (weighted blocking probability) constraints for a pre-defined time period (e.g. 24 hours), using knowledge of the traffic load profile and the energy harvesting statistics. The blocking probability is analyzed based on Erlang's approximation method [28] jointly considering the BSs' on-off states and the harvested energy profile.
- The grid power minimization problem is transformed into an unconstrained problem of minimizing a weighted combination of grid power consumption and blocking probability, which can be solved by a dynamic programming (DP) approach [9].
- A *two-stage DP algorithm*, which determines the BSs' on-off state in the first stage, and then optimizes per-BS resource allocation in the second stage, is proposed to reduce the computational complexity. The performance of the proposed algorithm is evaluated by

simulations and compared with the optimal DP algorithm and some heuristic algorithms.

The rest of the paper is organized as follows. Section II introduces the system model. The blocking probability is defined and analyzed in Section III. In Section IV, we study the average grid power minimization problem with a weighted blocking probability constraint. Numerical results are presented in Section V. Finally, Section VI concludes the paper.

II. System Model

We consider a wireless cellular system with a total of B BSs denoted as $\mathcal{B} = \{1, 2, \ldots, B\}$, each of which is powered jointly by an energy harvesting device and the power grid. The operational time line is divided into T time periods (e.g., $T = 24$ and the length of each time period is 1 hour). The models are detailed as follows.

A. Power Consumption Model

In time period t, the average harvested power of BS b is denoted by $P_{H,t}^{(b)}$, and the grid power is $P_{G,t}^{(b)}$. Assume a BS has the sufficiently large battery capacity for realistic operation conditions. For instance, a solar powered BS can store all the harvested energy during day-time. Hence, we do not consider battery overflow. The BS energy consumption in *active mode* is modeled as a constant power term plus a radio frequency (RF) related power [18], which is

$$P_{BS,t}^{(b)} = P_0 + \Delta_P P_{RF,t}^{(b)}, \tag{1}$$

where P_0 is the constant power including the baseband processor, the cooling system, and etc., Δ_P is the inverse of power amplifier efficiency factor, and $P_{RF,t}^{(b)}$ is the RF transmit power.

Assume the total wireless bandwidth W_0 is divided into N orthogonal subcarriers. The network will decide which BSs are powered on and how many subcarriers of these BSs are activated. The RF power is a linear function of the number of active subcarriers $n_t^{(b)}$, i.e.,

$$P_{RF,t}^{(b)} = \frac{n_t^{(b)}}{N} P_T, \quad n_t^{(b)} \leq N, \tag{2}$$

where P_T is the transmit power level. Based on the LTE standard [29], we assume a constant transmit power per-subcarrier in this work. Substituting $P^{(b)}_{RF,t}$ in (1) with (2), we get

$$P^{(b)}_{BS,t} = P_0 + \frac{n^{(b)}_t}{N} \Delta_P P_T. \tag{3}$$

Notice that we do not consider the power consumption of the broadcast, synchronization, and pilot channels, as it will just increase the total power consumption by a constant value.

In order to balance the performance among different time periods, the harvested energy may be reserved in the battery for future use by reducing the number of active subcarriers or by switching to *sleep mode*. In this paper, two types of sleep modes are considered. The first one is deep sleep mode, in which a BS is completely turned off for a time period. In this sleep mode, the BS power consumption is negligible and the users in the sleeping cell are served by the neighboring BSs. The second one is *opportunistic sleep mode*. An active BS will turn to this mode for a time ratio $\varphi^{(b)}_t \in [0, 1)$ to save grid energy. For example, if the traffic load is low and the renewable energy is insufficient, a larger value of $\varphi^{(b)}_t$ can be chosen to save more energy without causing too many blocking events. It can be realized by time domain BS sleep [30] where some subframes are turned off. In this mode, the users will be blocked due to lack of transmission subframes. We assume the power consumption in opportunistic sleep mode is P_S. Denote $S^{(b)}_t$ as the state of BS b at time t, which equals 1 if it is in active mode, and equals 0 otherwise. We summarise the BS power consumption model as:

$$P^{(b)}_{BS,t} = \begin{cases} P_0 + \frac{n^{(b)}_t}{N} \Delta_P P_T, & \text{if } S^{(b)}_t = 1, \\ P_S, & \text{if } S^{(b)}_t = 1 \text{ with opportunistic sleep}, \\ 0, & \text{if } S^{(b)}_t = 0. \end{cases} \tag{4}$$

In reality, a BS in sleep mode still consumes a certain amount of power so that it can be reactivated. However, the power to reactivate a BS is negligible compared with that in active mode. Hence, the sleep mode power consumption is approximated as zero.

B. Traffic Model

The users are sorted into groups according to their rate requirements and locations [31]. Assume there are K classes of users, each of which has a data rate requirement $R_k, k = 1, \ldots, K$. Based on the distance between users and BSs, the network is divided into M disjoint regions with equal areas, denoted by $A_m, m = 1, \ldots, M$. In each region m at time period t, the users from class k are uniformly distributed and randomly arrive according to a Poisson distribution with arrival rate $\lambda_{mk,t}$. The average service rate is denoted by μ_{mk}. Hence, the traffic intensity of user class k in area m is calculated by

$$\rho_{mk,t} = \frac{\lambda_{mk,t}}{\mu_{mk}}. \tag{5}$$

All the traffic in each area is served by the BS with largest signal strength. Once the BSs' active/sleep states are fixed, the serving BS for each user in each area is decided. The serving BS allocates bandwidth to users to meet their minimum rate requirement. Hence, a newly arrived user will be blocked if the available subcarriers are not sufficient to satisfy its rate requirement. The system can be viewed as a multi-server queue without user buffer, while the server capacity varies according to the users' channel states. Intuitively, when the network traffic load is high, more BSs and subcarriers should be active so that each BS takes care of a smaller area to guarantee the QoS. Otherwise, fewer BSs and subcarriers are required, and hence the power consumption can be reduced.

C. Channel Model

Since we aim to design the long time-scale policy, small-scale fast fading and shadowing are ignored assuming that they are averaged out for sufficient channel realizations. Hence, we mainly focus on distance-dependent pathloss effect, which facilitates the distance-based network division in the traffic model. The SINR of user u in the coverage area of active BS b is

$$\text{SINR}_u = \frac{P_T \Gamma (d_u^{(b)})^{-\alpha}}{\sigma^2 + \sum_{b': S^{(b')}=1, b' \neq b} \frac{n^{(b')}}{N} P_T \Gamma (d_u^{(b')})^{-\alpha}}, \tag{6}$$

where Γ is the pathloss constant, α is the pathloss exponent, $d_u^{(b)}$ is the distance between BS b and user u, and σ^2 is the noise power. We assume the $n^{(b)}$ subcarriers are randomly chosen from a total of N for every symbol transmission in each BS b, and are opportunistically allocated to users to meet their data rate requirements. As we do not assume any specific subcarrier scheduling mechanism, the interference is considered averaged over the whole bandwidth, i.e., the perceived interference power is scaled by the ratio of active subcarriers $\frac{n^{(b')}}{N}$. Then the maximum achievable transmission rate is

$$r_u = \frac{n^{(b)} W_0}{N} \log_2(1 + \text{SINR}_u). \tag{7}$$

Notice that as the data rate function is concave, the result based on our simplified assumption provides a lower bound for the performance in real systems. Short term packet level scheduling concerning shadowing, fast fading, and interference variation can be adopted to further improve the performance, which is left for future work. In the next section, we calculate the blocking probability as the QoS metric, and study the relationship between blocking probability and power.

III. Blocking Probability Analysis

The blocking probability is defined as the probability that a newly arrived user is blocked. In energy harvesting systems, a blocking event may be caused by two factors. The first one is a high traffic load which means that the required subcarriers are not available. We call it the *service blocking probability*. The second one is the BS's opportunistic sleep mode when the energy is not sufficient. Such a blocking probability is equal to the sleep ratio $\varphi_t^{(b)}$. As a user does not know what causes the blocking, we need to jointly consider these factors. This also allows the operator to trade the quality of service with energy consumption. We first analyze the service blocking probability, and then calculate the overall blocking probability. For simplicity, we ignore the index t in this section.

A. Service Blocking Probability

The service blocking probability is the the probability that a new call arriving to the BS is rejected because all resources are busy. As we evaluate the metric over a long enough time period (e.g., 1 hour), it can be obtained by the Erlang's formula [32]. We further extend the result to a multi-class scenario. Specifically, denote the instantaneous set of users of class k in area m by $\mathcal{U}_{mk}$, which are uniformly distributed in area m, and the user number by $U_{mk} = |\mathcal{U}_{mk}|$. We calculate the bandwidth requirement of user u of class k in area m by

$$\Phi_{mk}(u) = \frac{R_k}{r_u}, \tag{8}$$

which varies according to user's service rate R_k and location m. As each BS has a limited available bandwidth $\frac{n^{(b)}}{N} W_0$, the admission condition is that the total normalized bandwidth requirement should not exceed 1. Denote

$$z_b = \sum_{m \in \mathcal{M}^{(b)}} \sum_{k=1}^{K} \sum_{u \in \mathcal{U}_{mk}} \Phi_{mk}(u), \tag{9}$$

where $\mathcal{M}^{(b)}$ is the set of regions served by BS b, and BS b is assumed to be always active ($S^{(b)} = 1, \varphi^{(b)} = 0$). Hence, the service blocking probability can be expressed as

$$p_{\text{sv},mk} = \Pr(z_b < 1, z_b + \Phi_{mk}(u) \geq 1) \tag{10}$$

$$= \Pr(1 - \Phi_{mk}(u) \leq z_b < 1), \tag{11}$$

where (10) means that the total normalized bandwidth does not exceed 1 until a user u of class k arrives in area m. Calculation of the blocking probability (11) requires the integration of the probability over all the possible quantities and locations of users served by BS b, for which it is difficult to find analytical expressions. We make use of the *Erlang's approximation* method proposed in [28] and extend to our multi-class multi-area scenario. The basic idea of Erlang's approximation method is to average the users' bandwidth requirements over all the possible positions. Assuming that all the users in the area have the same bandwidth requirement, the blocking probability can be calculated by Erlang's formula [32]. Specifically, the average normalized bandwidth requirement of class k users in area m is

$$\bar{\Phi}_{mk} = \int_{A_m} \frac{R_k}{r_{u(a)} A_m} \mathrm{d}a. \tag{12}$$

where $r_{u(a)}$ is the achievable data rate of user u at position a, which is expressed as (7). Hence, the admission condition (9) is changed to

$$\sum_{m \in \mathcal{M}^{(b)}} \sum_{k=1}^{K} U_{mk} \bar{\Phi}_{mk} < 1, \tag{13}$$

where U_{mk} is the number of active users of class k in area m. At the same time, the blocking probability of a user of class k in area m is modified as

$$p_{\mathrm{sv},mk} = \Pr(1 - \bar{\Phi}_{mk} \leq \sum_{m' \in \mathcal{M}^{(b)}} \sum_{k'=1}^{K} U_{m'k'} \bar{\Phi}_{m'k'} < 1). \tag{14}$$

According to queueing theory (Sec. 3.7 [32] and Sec. 1.6 [33]), the stationary probability of active user state $\boldsymbol{U}^{(b)} = \{U_{mk}\}_{m \in \mathcal{M}^{(b)}, k=1,\ldots,K}$ associating to BS b is

$$\pi^{(b)}(\boldsymbol{U}^{(b)}) = \prod_{m \in \mathcal{M}^{(b)}} \prod_{k=1}^{K} \frac{\rho_{mk}^{U_{mk}}}{U_{mk}!} \left(\sum_{\boldsymbol{U}^{(b)} \in \mathcal{U}^{(b)}} \prod_{m \in \mathcal{M}^{(b)}} \prod_{k=1}^{K} \frac{\rho_{mk}^{U_{mk}}}{U_{mk}!} \right)^{-1}, \tag{15}$$

where ρ_{mk} is defined as (5), $\mathcal{U}^{(b)} = \{\boldsymbol{U}^{(b)} | \sum_{m \in \mathcal{M}^{(b)}} \sum_{k=1}^{K} U_{mk} \bar{\Phi}_{mk} < 1\}$ is the set of all possible active user states which satisfy the bandwidth constraint (13). As a consequence, the blocking probability can be calculated as

$$p_{\mathrm{sv},mk} = \sum_{\boldsymbol{U}^{(b)} \in \bar{\mathcal{U}}_{mk}^{(b)}} \pi^{(b)}(\boldsymbol{U}^{(b)}), \quad m \in \mathcal{M}^{(b)}, \tag{16}$$

where $\bar{\mathcal{U}}_{mk}^{(b)} = \{\boldsymbol{U}^{(b)} : 1 - \Phi_{mk} \leq \sum_{m' \in \mathcal{M}^{(b)}} \sum_{k'=1}^{K} U_{m'k'} \bar{\Phi}_{m'k'} \leq 1\}$ is the set of active user states where the newly arrived user of class k in area m is blocked. In addition, the probability that a newly arrived user in the coverage of BS b is blocked is

$$p_{\mathrm{sv}}^{(b)} = \frac{\sum_{m \in \mathcal{M}^{(b)}} \sum_{k=1}^{K} p_{\mathrm{sv},mk} \rho_{mk}}{\sum_{m \in \mathcal{M}^{(b)}} \sum_{k=1}^{K} \rho_{mk}} \tag{17}$$

Notice that the service blocking probability can be tuned by adapting the BSs' working states $S^{(b)}, b = 1, \ldots, B$ and the number of active subcarriers in the active BSs $n^{(b)}, b \in \{b : S^{(b)} = 1\}$.

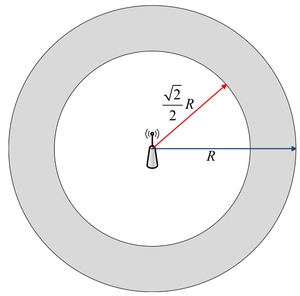

Fig. 1. Single-cell Erlang's approximation settings for $M = 2$.

Also notice that the partition of the M regions is not arbitrary, but based on the distance to the BSs to guarantee the approximation accuracy. Take a single cell case (Fig. 1) as an example. When $M = 2$, the cell edge users are grouped into one class, while the rests are in another. The example for the multi-cell case can be found in the simulation study. Further, increasing the value of M allows us to improve the approximation accuracy, while the computational complexity increases accordingly. Ideally, $M \to +\infty$ can yield the exact blocking probability, but the complexity is not affordable. The selection of M should balance approximation accuracy with computational complexity.

B. Relation between $P_G^{(b)}$ and $\varphi^{(b)}$

Recall that the BS in active mode can turn to opportunistic sleep mode with time ratio $\varphi^{(b)}$. Denote $P_{\text{In}}^{(b)}$ as the total input power. According to the balance between power input and consumption, we have

$$P_{\text{In}}^{(b)} = (1 - \varphi^{(b)}) P_{BS}^{(b)} + \varphi^{(b)} P_S, \quad P_{\text{In}}^{(b)} \leq P_{BS}^{(b)} \tag{18}$$

Then the relation between the opportunistic sleep time ratio and the input power is

$$\varphi^{(b)} = \frac{P_{BS}^{(b)} - P_{\text{In}}^{(b)}}{P_{BS}^{(b)} - P_S}. \quad P_{\text{In}}^{(b)} \leq P_{BS}^{(b)} \tag{19}$$

We now discuss the relationship between the opportunistic sleep time ratio and the grid power consumption according to the available harvested power.

1) Case 1: If the harvested energy is sufficient for the required energy, i.e., $E_C^{(b)} + P_H^{(b)} L \geq P_{\text{In}}^{(b)} L$, where $E_C^{(b)}$ is the battery energy budget, L is the length of a time period. Then we have

$$P_G^{(b)} = 0, \quad \forall\, 0 \leq \varphi^{(b)} \leq 1, \tag{20}$$

which means that the grid power input is not needed. Note that the updating process of battery energy $E_C^{(b)}$ is described in the next section.

2) Case 2: On the other hand, for the case where $E_C^{(b)} + P_H^{(b)} L < P_{\text{In}}^{(b)} L$, then grid power is needed. And the opportunistic sleep time ratio can be expressed as

$$\varphi^{(b)} = \frac{P_{BS}^{(b)} - (E_C^{(b)}/L + P_H^{(b)} + P_G^{(b)})}{P_{BS}^{(b)} - P_S}, \quad P_G^{(b)} \leq P_{BS}^{(b)} - (E_C^{(b)}/L + P_H^{(b)}). \tag{21}$$

C. Overall Blocking Probability

In our system, if the BS is in opportunistic sleep mode, a newly arrived user of class k in area m served by BS b will be blocked with probability 1. Otherwise, it will be blocked with probability $p_{\text{sv},mk}$. As a consequence, the overall blocking probability can be calculated as

$$\begin{aligned} p_{\text{blk},mk} &= \varphi^{(b)} + (1 - \varphi^{(b)}) p_{\text{sv},mk} \\ &= 1 - (1 - p_{\text{sv},mk})(1 - \varphi^{(b)}). \end{aligned} \tag{22}$$

If we focus on the blocking probability for BS b, then we have

$$\begin{aligned} p_{\text{blk}}^{(b)} &= \frac{\sum_{m \in \mathcal{M}^{(b)}} \sum_{k=1}^{K} p_{\text{blk},mk} \rho_{mk}}{\sum_{m \in \mathcal{M}^{(b)}} \sum_{k=1}^{K} \rho_{mk}} \\ &= 1 - (1 - p_{\text{sv}}^{(b)})(1 - \varphi^{(b)}), \end{aligned} \tag{23}$$

where $p_{\text{sv}}^{(b)}$ is expressed as (17). Notice that if BS b is in sleep mode ($S^{(b)} = 0$), the users in the sleeping cell must be associated with the other active BSs. Hence, no blocking events are counted for this sleeping BS.

IV. Power Grid Energy Minimization

Recall that our objective is to reduce the carbon emissions in the cellular networks with mixed power supply by fully utilizing renewable energy. The problem can be formulated as minimizing the grid power consumption under the users' QoS constraint. This section presents the mathematical formulation and the solutions of the problem in detail.

A. Problem Formulation

In this section, we formulate the grid power minimization problem. The traffic intensity in time period t for the K classes of users and M regions is denoted by an $M \times K$ matrix $\boldsymbol{\rho}_t = \{\rho_{mk,t}\}_{m=1,\ldots,M,k=1,\ldots,K}$. The energy harvesting power is denoted by a $1 \times B$ vector $\boldsymbol{P}_{\boldsymbol{H},t} = [P_{H,t}^{(1)}, P_{H,t}^{(2)}, \ldots, P_{H,t}^{(B)}]$. The traffic profile $\boldsymbol{\rho}_t$ and the renewable energy profile $\boldsymbol{P}_{\boldsymbol{H},t}$ are assumed to be non-causally known. By adjusting the BSs' on-off states $\boldsymbol{S}_t = [S_t^{(1)}, S_t^{(2)}, \ldots, S_t^{(B)}]$, the number of active subcarriers of active BSs $\boldsymbol{n}_t = [n_t^{(1)}, n_t^{(2)}, \ldots, n_t^{(B)}]$, and the opportunistic sleep time ratio $\boldsymbol{\varphi}_t = [\varphi_t^{(1)}, \varphi_t^{(2)}, \ldots, \varphi_t^{(B)}]$, we can adapt the grid power input as well as the total power usage in all the time periods $t = 1, 2, \ldots, T$.

Denote $\boldsymbol{S} = \{\boldsymbol{S}_1, \boldsymbol{S}_2, \ldots, \boldsymbol{S}_T\}, \boldsymbol{n} = \{\boldsymbol{n}_1, \boldsymbol{n}_2, \ldots, \boldsymbol{n}_T\}, \boldsymbol{\varphi} = \{\boldsymbol{\varphi}_1, \boldsymbol{\varphi}_2, \ldots, \boldsymbol{\varphi}_T\}$, Then the following optimization problem is considered: given the traffic profile $\boldsymbol{\rho}_1, \boldsymbol{\rho}_2, \ldots, \boldsymbol{\rho}_T$ and the renewable energy profile $\boldsymbol{P}_{\boldsymbol{H},1}, \boldsymbol{P}_{\boldsymbol{H},2}, \ldots, \boldsymbol{P}_{\boldsymbol{H},T}$, adjust the BSs' working state $\boldsymbol{S}$, the resource allocation $\boldsymbol{n}$ and the sleep ratio $\boldsymbol{\varphi}$ to minimize the average grid power consumption while satisfying the weighted blocking probability. The problem can be formulated as

$$\min_{\boldsymbol{S},\boldsymbol{n},\boldsymbol{\varphi}} \quad \frac{\sum_{t=1}^{T} L_t \sum_{b=1}^{B} P_{G,t}^{(b)}}{\sum_{t=1}^{T} L_t} \tag{24}$$

$$\text{s.t.} \quad \sum_{t=1}^{T} \sum_{b=1}^{B} \omega_t^{(b)} p_{\text{blk},t}^{(b)} \le p_{\text{target}}, \tag{25}$$

where L_t denotes the length of time period t, the blocking probability $p_{\text{blk},t}^{(b)}$ is expressed as (23), and the weighting factor $\omega_t^{(b)}$, which satisfies $\sum_{t=1}^{T} \sum_{b=1}^{B} \omega_t^{(b)} = 1$, reflects the system sensitivity to the blocking probability in each time period. The weighting factor allows for the case where users may require higher QoS at some particular times of the day. For instance, if higher QoS is required during peak load times (e.g. day time) than low load times (e.g. night time), we can set the weighting factor for the day time to be larger than that for night time. The influence of the weighting factor settings is studied in the simulations. Considering the weighted blocking probability instead of a per-BS blocking constraint, we can trade the QoS with the energy reduction by sacrificing some QoS in low traffic regime more flexibly, which has little influence to the overall QoS. In addition, such a relaxed constraint also helps simplify the problem formulation.

Note that the solution for the problem (24) is not straightforward as the network traffic profile and the renewable energy profile in both time and space domain do not match with each other in general. We cannot just greedily use renewable energy as long as it is available, and then use grid energy if necessary. Storing some renewable energy for future use may reduce the overall grid power consumption. Also notice that we only consider a time-averaged grid power consumption. This model can also be used to solve the problem where the cost of grid power varies with time. For example, by simply substituting the per-time period weight of grid power $L_t/(\sum_{t=1}^{T} L_t)$ with electricity price, we can minimize the charge for electricity.

B. Optimal DP Algorithm

The optimal solution for the problem (24) with the constraint (25) can be found by exhaustive search through all possible policies. However, this approach is not practical due to its high complexity. We consider the following unconstrained optimization problem with a weighted combination of the power consumption and the blocking probability

$$\min_{\boldsymbol{S},\boldsymbol{n},\boldsymbol{\varphi}} \frac{\sum_{t=1}^{T} L_t \sum_{b=1}^{B} P_{G,t}^{(b)}}{\sum_{t=1}^{T} L_t} + \beta \sum_{t=1}^{T} \sum_{b=1}^{B} \omega_t^{(b)} p_{\mathrm{blk},t}^{(b)}, \tag{26}$$

where the factor $\beta > 0$ plays the role of a Lagrangian multiplier and can be chosen to set the relative importance of the blocking probability with respect to the average grid power consumption. Denote the minimum objective value of problem (26) for a given β as $P^*_{G\mathrm{ave},\beta} + \beta p^*_{\mathrm{blk},\beta}$, where $P^*_{G\mathrm{ave},\beta}$ and $p^*_{\mathrm{blk},\beta}$ represent the average grid power and the weighted blocking probability, respectively. By solving the problem (26) for different value of β, we can find a set of points $(P^*_{G\mathrm{ave},\beta}, p^*_{\mathrm{blk},\beta})$. Denote the function $P_{G\mathrm{ave}}(p^*_{\mathrm{blk},\beta}) = P^*_{G\mathrm{ave},\beta}$. The following theorem shows the relationship between the unconstrained problem and the original constrained problem, i.e., the solution of the problem (26) is also the solution of the problem (24) with the constraint (25).

Theorem 1. *Define the optimal objective function of (24) as*

$$P_{G\mathrm{ave,min}} = \min_{\boldsymbol{S},\boldsymbol{n},\boldsymbol{\varphi}} \frac{\sum_{t=1}^{T} L_t \sum_{b=1}^{B} P_{G,t}^{(b)}}{\sum_{t=1}^{T} L_t} \tag{27}$$

satisfying (25). If $p_{\mathrm{target}} = p^*_{\mathrm{blk},\beta}$*, we have* $P_{G\mathrm{ave,min}} = P^*_{G\mathrm{ave},\beta}$.

Proof: Firstly, the policy achieving $(P^*_{G\mathrm{ave},\beta}, p^*_{\mathrm{blk},\beta})$ of problem (26) is a feasible policy for problem (24) with the constraint (25). Hence,

$$P_{G\mathrm{ave,min}} \leq P^*_{G\mathrm{ave},\beta} \tag{28}$$

Secondly, the equality in (28) always holds as otherwise, we have

$$P_{G\mathrm{ave,min}} + \beta p^*_{\mathrm{blk},\beta} < P^*_{G\mathrm{ave},\beta} + \beta p^*_{\mathrm{blk},\beta}, \tag{29}$$

which contradicts the optimality of $(P^*_{G\mathrm{ave},\beta}, p^*_{\mathrm{blk},\beta})$ for problem (26). ■

Depending on Theorem 1, as the objective (26) is minimized, $P^*_{G\mathrm{ave},\beta}$ must be the minimum average grid power to guarantee that the blocking probability is no more than $p^*_{\mathrm{blk},\beta}$. Hence, the solution for (26) is also the one for (24) where $p_{\mathrm{target}} = p^*_{\mathrm{blk},\beta}$. Hence, $P_{G\mathrm{ave}}(p_{\mathrm{blk}})$ indicates the minimum average grid power such that the blocking probability does not exceed p_{blk}. Notice that it is not guaranteed that all the values of $P_{G\mathrm{ave}}(p_{\mathrm{blk}})$ can be found by varying β. In this case, for a given target blocking probability p_{target}, if a corresponding point can be found by setting an appropriate value of β, the optimal solution for the original problem (24) with constraint (25) is found. Otherwise, we can just get a suboptimal result by adopting the policy related to the point with the largest blocking probability less than p_{target}, i.e.,

$$\{\boldsymbol{S}, \boldsymbol{n}, \boldsymbol{\varphi}\} = \arg\max\{p^*_{\text{blk},\beta} | p^*_{\text{blk},\beta} \leq p_{\text{target}}\}. \tag{30}$$

The problem (26) can be solved by the DP approach for deterministic systems (Chap. 2, [9]), which divides the whole problem into simple per-stage sub-problems, so DP is a candidate approach to find the optimal policy. The DP algorithm contains three key components: state, action and cost function. In the problem (26), the state is the amount of energy $\boldsymbol{E}_{C,t} = [E^{(1)}_{C,t}, E^{(2)}_{C,t}, \ldots, E^{(B)}_{C,t}]$ in the battery at the beginning of time period t. For each BS b, $E^{(b)}_{C,t}$ evolves to time period $t+1$ as

$$E^{(b)}_{C,t+1} = E^{(b)}_{C,t} + L_t P^{(b)}_{H,t} - \left[\left(1 - \varphi^{(b)}_t\right) L_t P^{(b)}_{BS,t} + \varphi^{(b)}_t L_t P_S\right] \tag{31}$$

if the energy consumption in time period t does not exceed the available renewable energy, i.e.,

$$\left[\left(1 - \varphi^{(b)}_t\right) L_t P^{(b)}_{BS,t} + \varphi^{(b)}_t L_t P_S\right] \leq E^{(b)}_{C,t} + L_t P^{(b)}_{H,t}. \tag{32}$$

If the harvested energy is not sufficient, i.e., (32) does not hold, the power grid will plug in to provide the required power. The grid power is selected as

$$P^{(b)}_{G,t} \leq \max\left\{0, (1 - \varphi^{(b)}_t) P^{(b)}_{BS,t} + \varphi^{(b)}_t P_S - \frac{E^{(b)}_{C,t}}{L_t} - P^{(b)}_{H,t}\right\}. \tag{33}$$

The actions are the BSs' working state $\boldsymbol{S}_t$, the number of active subcarriers $\boldsymbol{n}_t$, and the sleep ratio $\boldsymbol{\varphi}_t$. Notice that if $S^{(b)}_t = 0$, there are no active subcarriers ($n^{(b)}_t = 0$), and the BS remains asleep during t ($\varphi^{(b)}_t = 1$). The per-stage cost is the weighted combination of the grid power and the blocking probability, denoted as a function of the current action and state

$$c_t(\boldsymbol{S}_t, \boldsymbol{n}_t, \boldsymbol{\varphi}_t, \boldsymbol{E}_{C,t}) = \frac{L_t \sum_{b=1}^{B} P^{(b)}_{G,t}}{\sum_{t=1}^{T} L_t} + \beta \sum_{b=1}^{B} \omega^{(b)}_t p^{(b)}_{\text{blk},t}. \tag{34}$$

The DP algorithm breaks the original problem down into sub-problems with respect to the stage, where the objective is to minimize the cost of each time period plus that of the following time periods. The per-time period sub-problems are solved recursively. The *cost-to-go* function is defined recursively as

$$J_t(\boldsymbol{E}_{C,t}) = \begin{cases} \min\limits_{\boldsymbol{S}_t,\boldsymbol{n}_t,\boldsymbol{\varphi}_t} c_t(\boldsymbol{S}_t,\boldsymbol{n}_t,\boldsymbol{\varphi}_t,\boldsymbol{E}_{C,t}), & t=T \\ \min\limits_{\boldsymbol{S}_t,\boldsymbol{n}_t,\boldsymbol{\varphi}_t} \{c_t(\boldsymbol{S}_t,\boldsymbol{n}_t,\boldsymbol{\varphi}_t,\boldsymbol{E}_{C,t})+J_{t+1}(\boldsymbol{E}_{C,t+1})\}, & t<T \end{cases} \tag{35}$$

which denotes the minimum cost of the sub-problem with time period t as its initial stage. Performing a backward induction of the cost-to-go functions (35) from time period T to time period 1, we can obtain the minimum cost equal to $J_1(\mathbf{0})$.

Assume the number of examined sleep ratios $\varphi_t^{(b)}$ is N_φ. Then, the cardinality of the action space for each cost-to-go function is $(NN_\varphi+1)^B$. Note that the number of BS actions $(S_t^{(b)}, n_t^{(b)}, \varphi_t^{(b)})$ is $(NN_\varphi+1)$ instead of $2NN_\varphi$, as the BSs in sleep mode have only a single state. Hence, given the state in time period t, the cardinality of the state space in time period $(t+1)$ is no more than $(NN_\varphi+1)^B$. That is, if the harvested energy of all BSs is enough for any resource allocation policy, each policy corresponds to a unique next-stage state. Otherwise, some policies result in the same state, so the state space is less than $(NN_\varphi+1)^B$.

Both the action space and the state space dimensions increase exponentially with the number of BSs B in the network, which, due to the *curse of dimensionality* [9], will result in an overwhelming computational complexity to find the optimal control policy if the network size is large. As a consequence, the proposed DP optimal algorithm is difficult to implement in practical systems, and low-complexity solutions are required. In the following, a two-stage optimization algorithm is proposed to reduce the size of the state and action space.

C. Two-stage DP Algorithm

The basic idea of the two-stage optimization algorithm is to divide the action process into two steps. In the first stage, we assume that the number of active subcarriers in active BSs are always N, i.e., subcarrier allocation is not considered in this stage. In addition, the active BS sleep ratio $\varphi_t^{(b)}$ is assumed to be 0 for all the $b=1,\ldots,B$, which means the required power is always available. As a result, the actions at this stage only consist of the BSs' working states $\boldsymbol{S}$. The optimization problem can be written as

$$\min_{\boldsymbol{S}} \frac{\sum_{t=1}^{T} L_t \sum_{b=1}^{B} P_{G,t}^{(b)}}{\sum_{t=1}^{T} L_t} + \beta \sum_{t=1}^{T} \sum_{b=1}^{B} \omega_t^{(b)} p_{\text{blk},t}^{(b)} \Big|_{\boldsymbol{n}_t=\boldsymbol{n}_0, \boldsymbol{\varphi}_t=\boldsymbol{\varphi}_0, \forall t}, \tag{36}$$

where $\boldsymbol{n}_0 = [n_0^{(1)}, \ldots, n_0^{(B)}], \boldsymbol{\varphi}_0 = [\varphi_0^{(1)}, \ldots, \varphi_0^{(B)}]$ are the given initial states. It can be set by *greedy initial state settings* expressed as $\boldsymbol{n}_0 = \boldsymbol{N}, \boldsymbol{\varphi}_0 = \boldsymbol{0}$, i.e., for any $b = 1, 2, \ldots, B$, if $S_t^{(b)} = 1$, the corresponding number of active subcarriers is $n_t^{(b)} = N$, and the sleep ratio is $\varphi_t^{(b)} = 0$, i.e., BS b activates all the subcarriers for the whole time period t. Other settings will be discussed later in the simulations. The cost-to-go function is

$$\begin{aligned} & J_t(\boldsymbol{E}_{C,t})|_{\boldsymbol{n}_t=\boldsymbol{n}_0, \boldsymbol{\varphi}_t=\boldsymbol{\varphi}_0} \\ &= \begin{cases} \min\limits_{\boldsymbol{S}_t} c_t(\boldsymbol{S}_t, \boldsymbol{n}_0, \boldsymbol{\varphi}_0, \boldsymbol{E}_{C,t}), & t = T \\ \min\limits_{\boldsymbol{S}_t} \left\{ c_t(\boldsymbol{S}_t, \boldsymbol{n}_0, \boldsymbol{\varphi}_0, \boldsymbol{E}_{C,t}) + J_{t+1}(\boldsymbol{E}_{C,t+1})|_{\boldsymbol{n}_{t+1}=\boldsymbol{n}_0, \boldsymbol{\varphi}_{t+1}=\boldsymbol{\varphi}_0} \right\}, & t < T \end{cases} \end{aligned} \tag{37}$$

Remark 1: The action space of each cost-to-go function in (37) is 2^B. Given the state in time period t, the maximum state space in time period $(t+1)$ is reduced from $(NN_\varphi + 1)^B$ to 2^B.

The problem (36) can be solved by the standard DP algorithm with a much lower complexity compared to the original DP problem (26). In the second stage, given the BSs' working state $\boldsymbol{S}^* = \{\boldsymbol{S}_1^*, \boldsymbol{S}_2^*, \ldots, \boldsymbol{S}_T^*\}$ obtained from the first stage, we adjust the number of active subcarriers and power allocation for each BS separately. Since the subcarrier adaptation changes the interference profile, the per-BS resource allocation correlates with one another. We propose an iterative resource allocation algorithm, which updates the per-BS resource allocation based on the allocation results of the other BSs, and then iterates the process until the resource allocation solution does not change between two consecutive iterations. The per-BS resource allocation optimization problem can be formulated as

$$\min_{n_t^{(b)}, \varphi_t^{(b)}} \frac{\sum_{t=1}^{T} L_t \sum_{b=1}^{B} P_{G,t}^{(b)}}{\sum_{t=1}^{T} L_t} + \beta \sum_{t=1}^{T} \sum_{b=1}^{B} \omega_t^{(b)} p_{\text{blk},t}^{(b)} \Big|_{\boldsymbol{S}^*, n_t^{(b')}, \varphi_t^{(b')}, \forall t, b' \neq b}. \tag{38}$$

The problem can also be solved by the DP algorithm where the cost-to-go function is

$$J_t^{(b)}(E_{C,t}^{(b)})|_{\boldsymbol{S}_t^*,n_t^{(b')},\varphi_t^{(b')},b'\neq b}$$
$$=\begin{cases}\min\limits_{n_t^{(b)},\varphi_t^{(b)}} c_t(\boldsymbol{S}_t=\boldsymbol{S}_t^*,\boldsymbol{n}_t^{(b)},\boldsymbol{\varphi}_t^{(b)},\boldsymbol{E}_{C,t}^{(b)})|_{n_t^{(b')},\varphi_t^{(b')},b'\neq b}, & t=T\\ \min\limits_{n_t^{(b)},\varphi_t^{(b)}} \left\{c_t(\boldsymbol{S}_t=\boldsymbol{S}_t^*,\boldsymbol{n}_t^{(b)},\boldsymbol{\varphi}_t^{(b)},\boldsymbol{E}_{C,t}^{(b)})|_{n_t^{(b')},\varphi_t^{(b')},b'\neq b}+J_{t+1}(\boldsymbol{E}_{C,t+1})|_{\boldsymbol{S}_t^*,n_{t+1}^{(b')},\varphi_{t+1}^{(b')},b'\neq b}\right\}, & t<T\end{cases} \tag{39}$$

Remark 2: The action space of each cost-to-go function in (39) is either NN_φ ($S_t^{(b)*}=1$) or 1 ($S_t^{(b)*}=0$), and given the state in time period t, the maximum state space in time period $(t+1)$ is no more than NN_φ.

Remark 3: With the two-stage algorithm, the action space of each time period optimization is reduced from $(NN_\varphi+1)^B$ to $2^B BNN_\varphi$. Accordingly, given the state in time period t, the maximum state space in time period $(t+1)$ is reduced from $(NN_\varphi+1)^B$ to $2^B BNN_\varphi$.

Algorithm 1 Two-stage DP Optimization

The 1st stage:

Solve the problem (36) to find $\boldsymbol{S}^*$.

The 2nd stage:

Set $\boldsymbol{n}_t=\boldsymbol{n}_0,\boldsymbol{\varphi}_t=\boldsymbol{\varphi}_0,\boldsymbol{n}_t'\neq\boldsymbol{n}_t,\boldsymbol{\varphi}_t'\neq\boldsymbol{\varphi}_t,t=1,\ldots,T$

while $\boldsymbol{n}_t\neq\boldsymbol{n}_t'$ or $\boldsymbol{\varphi}_t\neq\boldsymbol{\varphi}_t'$ for some $t=1,\ldots,T$ **do**

  Set $\boldsymbol{n}_t'=\boldsymbol{n}_t,\boldsymbol{\varphi}_t'=\boldsymbol{\varphi}_t,t=1,\ldots,T$.

  for $b=1$ to N **do**

    Set $\boldsymbol{n}^{(b)}=\{n_1^{(b)},n_2^{(b)},\ldots,n_T^{(b)}\},\boldsymbol{\varphi}^{(b)}=\{\varphi_1^{(b)},\varphi_2^{(b)},\ldots,\varphi_T^{(b)}\}$

    Find $\boldsymbol{n}^{(b)*},\boldsymbol{\varphi}^{(b)*}$ which solve the problem (38) by fixing $\boldsymbol{n}^{(b')}$ and $\boldsymbol{\varphi}^{(b')},b'\neq b$.

    Update $\boldsymbol{n}_t,\boldsymbol{\varphi}_t,t=1,\ldots,T$ by setting $\boldsymbol{n}^{(b)}=\boldsymbol{n}^{(b)*},\boldsymbol{\varphi}^{(b)}=\boldsymbol{\varphi}^{(b)*}$.

  end for

end while

The algorithm is summarized as Algorithm 1. Notice that the proposed two-stage DP algorithm may not achieve the optimal solution in general. However, its performance can be guaranteed when the traffic is uniformly distributed in space domain and the energy arrival process in each BS is the same. In this case, to match the resource allocation with traffic and efficiently utilize energy, each active BS activates all its subcarriers. As a result, the two-stage DP algorithm performs the same with the optimal DP algorithm. Both of them just need to optimize optimal BS sleeping policy as the 1st stage DP algorithm. The result is summarized as the following proposition.

Proposition 1. *If for any* t*, we have* $\rho_{mk,t} = \tilde{\rho}_t, \forall m = 1, \ldots, M, k = 1, \ldots, K, P_{H,t}^{(1)} = \ldots = P_{H,t}^{(B)}$*, the performance of two-stage DP algorithm is the same with that of optimal DP algorithm.*

For simplicity, we present the outline of the proof which can be divided into three steps. First, it can be proved that the blocking probability $p_{\text{blk},t}^{(b)}$ is a convex function of the traffic covered by BS b. Hence, the average blocking probability $\sum_{b=1}^{B} \omega_t^{(b)} p_{\text{blk},t}^{(b)}$ is minimized when the active BSs evenly share the network traffic. As we assume the distance based association, uniform BS sleeping can guarantee even load sharing. Secondly, for a given grid power consumption, the total number of active subcarriers is fixed. In this case, the network capacity is maximized when $n_t^{(b)} = \tilde{n}, \forall b : S_t^{(b)} = 1$ according to (6) and (7) due to the concavity of the rate function, and the average blocking probability is then minimized. Finally, we state that $\tilde{n} = N$ as in this case, the ratio between transmit power and fixed power of all the BSs is maximized. Hence, the energy is most efficiently used to achieve the minimum blocking probability.

The result is further validated by simulation results later. The simulations also show that in some other cases, for example an asymmetric traffic distribution, the performance of two-stage DP algorithm can not be guaranteed to achieve the optimal result.

D. Heuristic Algorithms

Motivated by the two-stage DP algorithm where the BSs' on-off states are determined in the first stage, and the per-BS resource allocation is determined in the second stage, we propose some low-complex heuristic algorithms for comparison, which also operates in a two-stage manner. Specifically, the BSs' on-off states can be adjusted by the following algorithms:

- *Non-sleep policy*. In this policy, all the BSs are active in each time period. It is the policy used in the traditional cellular network, which can be viewed as a baseline strategy.
- *Threshold-based sleep policy*. In this policy, the number of active BSs are decided by the network traffic intensity. Assume the maximum supportable traffic is $\theta_{\max}$. We set Q BSs' on-off patterns, in each of which $B_{\min} + iB_q$ uniformly chosen BSs are active, where $B_{\min}$ is the minimum number of active BSs required to guarantee the network coverage, and B_q is an integer satisfying $B_{\min} + QB_q \leq B$. We define a set of thresholds $0 = \theta_0 < \theta_1 < \ldots < \theta_Q = \theta_{\max}$. If the integrated network traffic intensity satisfies $\theta_{i-1} < \sum\limits_m \sum\limits_k \rho_{mk} \leq \theta_i$, the i-th pattern is chosen.

Once the BSs' on-off states are decided, the number of active subcarriers and the opportunistic sleep ratio are tuned in each BS individually based on the algorithms listed below:

- *Maximum resource block utilization*. In this policy, all the blocks are activated for transmission, i.e., $n_t^{(b)} = N$ for all t. It can be considered as a baseline case.
- *Traffic-aware resource block utilization*. Based on the intuition that higher traffic intensity requires more wireless resources, we propose a policy where the number of activated subcarriers is set proportional to the traffic intensity, i.e.,

$$n_t^{(b)} = \min\{N, \lceil \eta_1 \rho_t^{(b)} N \rceil\}, \quad \eta_1 > 0 \tag{40}$$

  where $\lceil x \rceil$ is the minimum integer no smaller than x, and $\rho_t^{(b)}$ is the aggregated traffic intensity of BS b.

- *Joint traffic-energy-aware resource block utilization.* As the outages are caused not only by the lack of wireless resources, but also by the lack of power, the power budget should be taken into consideration. In this case, the number of active subcarriers is also proportional to the available power besides the traffic intensity:

$$n_t^{(b)} = \min\left\{N, \left\lceil \eta_2 \rho_t^{(b)} \frac{E_{B,t}^{(b)} + E_{G,t}^{(b)} + L_t P_{H,t}^{(b)}}{\sum_{k=t}^{T} L_k (P_0 + \Delta_P P_T)} N \right\rceil \right\}, \tag{41}$$

where $\eta_2 > 0$. As the grid energy can be used flexibly, given the average grid power $P_{G\mathrm{ave}}^{(b)}$, we view the grid energy as a virtual battery with initial state $E_{G,1}^{(b)} = \sum_{t=1}^{T} L_t P_{G\mathrm{ave}}^{(b)}$ which evolves as $E_{G,t+1}^{(b)} = \max\{0, E_{G,t}^{(b)} - L_t P_{G,t}^{(b)}\}$. Note that $P_0 + \Delta_P P_T$ in the denominator is for normalization.

The sleep ratio $\varphi_t^{(b)}$ in all these policies is set zero as long as the required power is available either from energy harvesting or from power grid. Hence, the grid power is calculated as

$$P_{G,t}^{(b)} = \min\left\{ \frac{E_{G,t}^{(b)}}{L_t}, \max\left\{0, P_0 + \frac{n_t^{(b)}}{N} \Delta_P P_T - \frac{E_{B,t}^{(b)}}{L_t} - P_{H,t}^{(b)} \right\} \right\}, \tag{42}$$

and $\varphi_t^{(b)} > 0$ only when the total energy is not sufficient.

Notice that given the parameters θ_i, η_1, η_2, the heuristic algorithms only depend on the traffic and the energy conditions of current time period. The complexity is much lower than the DP algorithm. However, the QoS performance is not guaranteed, which is shown in the simulation results in the next section.

V. Numerical Simulations

We adopt the energy consumption model of the macro BS from the EARTH project [18], and the channel model from 3GPP LTE [29] for numerical simulations. In the macro-cell scenario, we have $P_0 = 712.2$W, $\Delta_P = 15.96$, the maximum transmit power $P_{\max} = 40$W, and the cell radius $R = 1000$m. The opportunistic sleep mode power is $P_S = 50$W. The bandwidth is set to $W_0 = 10$MHz and the number of sub-carriers is set to $N = 600$. The path-loss is $\mathrm{PL}^{\mathrm{dB}} = 34.5 + 35\log_{10}(l)$, and the noise power density is -174dBm/Hz. We first study the

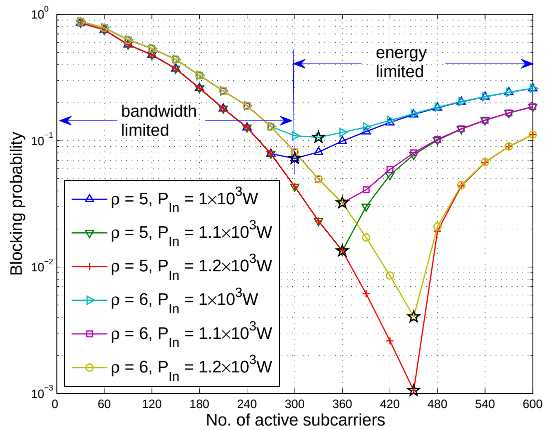

Fig. 2. Relationship between blocking probability and number of active subcarriers. ρ is the traffic intensity, P_{In} is the total input power available. The "star" is the minimum blocking probability for each parameter settings.

relation between the QoS and the resource allocation in single cell scenario, and evaluate the proposed DP algorithm in this setup. Then the simulation is extended to sectorized multi-cell scenario to study the performance of the two-stage DP algorithm.

A. *Single-Cell Case*

For the single-cell case, the superscript b is ignored for simplicity. We set the number of user classes as $K = 1$. The circular cell area are divided into $M = 2$ regions with equal areas, as shown in Fig. 1. It is easy to find that the inner circular region is of radius of $\frac{\sqrt{2}}{2}R$. Accordingly, the user data requirement is $r_K = r_0 = 2$Mbps, the user service rate is $\mu_{1K} = \mu_{2K} = \mu = 1\text{s}^{-1}$, and the arrival rate $\lambda_{1K} = \lambda_{2K} = \frac{\lambda}{2}$. The total traffic intensity is denoted by $\rho = \lambda/\mu$, and the total input power is denoted by P_{In}, which includes harvested power, grid power and battery power. The relation between the number of active subcarriers and the blocking probability is depicted in Fig. 2. Take $\rho = 5, P_{\text{In}} = 1 \times 10^3 W$ as an example. When the number of active subcarriers is less than 300, the blocking is mainly caused by the limited availability of subcarriers. Hence, the region where $n < 300$ is called the *bandwidth limited* region. On the contrary, if $n \geq 300$,

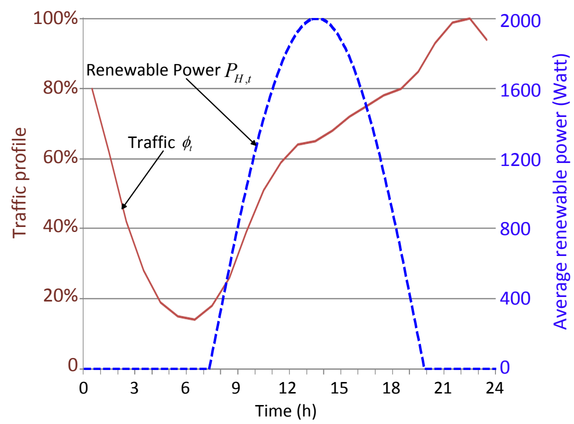

Fig. 3. Daily traffic (solid line) [18] and renewable energy profile (dashed line) [19].

the available power is insufficient to enable the active subcarriers to be always on, which means $\varphi > 0$. Then the blocking is also caused by opportunistic sleep, which gradually becomes the main blocking factor. Correspondingly, the region where $n \geq 300$ is called the *energy limited* region. As a result, there is a minimum outage probability working point as shown by the star on each curve. In addition, if a certain blocking probability can be achieved in both bandwidth limited region and energy limited region, the policy in bandwidth limited region consumes less power than P_{In}, while that in energy limited region consumes all the available power P_{In}. Hence, when achieving the same blocking probability, conservative subcarrier activation without violating the power constraint to avoid sleep is more energy efficient than aggressive subcarrier activation with opportunistic sleeping. In the following simulation, we only consider subcarrier adaptation in the bandwidth limited region, i.e., we set $\varphi = 0$ for all the conditions.

Then the performance of the DP algorithm to minimize the grid energy consumption is evaluated with a given traffic profile and energy arrival statistics for one day. We run the standard DP algorithm (35) for the single-cell case as the computational complexity is affordable. The traffic profile and renewable energy harvesting profile are taken from [18] and [19], respectively, as shown in Fig. 3. We set $T = 24$, and the length of each time period is $L_t = 1$ hour. The traffic

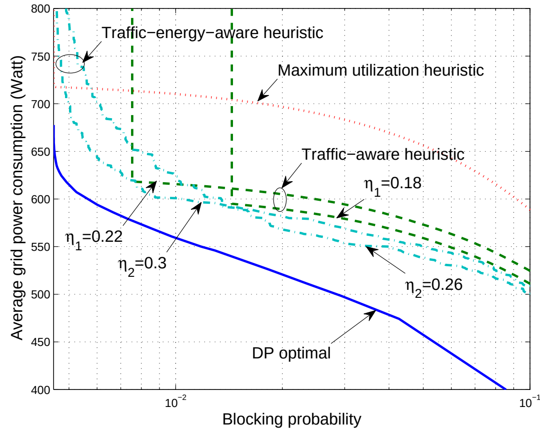

Fig. 4. Tradeoff curves between outage probability and grid energy consumption with different policies.

profile is $\lambda_t = \phi_t \lambda_{\max}$, where the maximum traffic intensity $\lambda_{\max} = 10\text{s}^{-1}$ and $0 < \phi_t \leq 1$.

The tradeoff between average blocking probability ($\omega_t = 1/T$) and grid energy consumption for different policies is depicted in Fig. 4. The joint traffic-energy-aware policy performs better than the traffic-aware policy in almost all conditions by choosing a proper value of η_2 ($\eta_2 = 0.26, 0.3$ for $\eta_1 = 0.18, 0.22$, respectively). In addition, by adjusting the value of η_1 and η_2, we obtain different curves. For instance, the traffic-aware heuristic algorithm with a smaller value of η_1 (0.18) performs closer to the optimal than that with larger value (0.22) for the low grid power input regime (< 610 Watt), and that with larger η_1 (0.22) is near optimal for the high grid energy input regime (> 610 Watt). Notice that there is a sudden change point on traffic-aware algorithm curve. The left part of the change point is not achievable is because that the number of active subcarriers is fixed for given traffic load in this algorithm, even though there is additional energy.

Fig. 5 shows the per-time period blocking performance of the DP algorithm for the same average blocking probability target (1%). In this simulation, we set $\omega_t = \phi_t^j / \sum_t \phi_t^j$. Note that ϕ_t^j is the j-th power of ϕ_t, where $\phi_t = \lambda_t/\lambda_{\max}$ is the ratio between the instantaneous traffic and

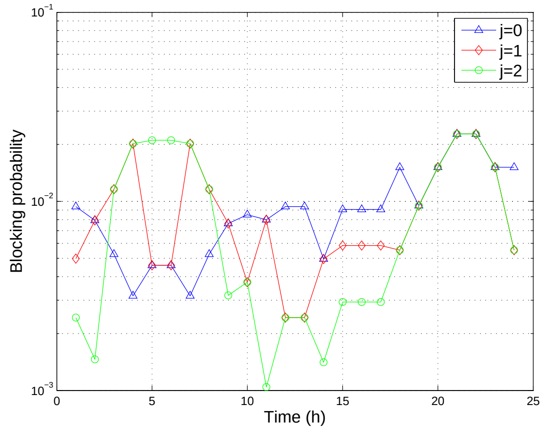

Fig. 5. Per-time period outage probability with different weighting factors $\omega_t = \phi_t^j / \sum_t \phi_t^j$. The average outage probability is identical as 1%.

the maximum traffic, and the exponent takes values $j = 0, 1, 2$. Different values of j indicate different weights for blocking probability. The exponent $j = 0$ corresponds to the average blocking probability, and $j = 1$ means traffic weighted blocking. As $\phi_t < 1$, larger j implies a higher weight for the high traffic regime. It can be seen that by adjusting the weighting factor, we can obtain different blocking profiles. Specifically, the algorithm tends to increase the blocking probability in a low traffic load regime if the corresponding weighting factor is large ($j = 2$).

B. 3-Sector Case

We now turn to multi-cell scenario. We consider the sectorized multi-cell setup as shown in Fig. 6(a), where each cite has 3 co-located BSs. In this setup, the dominant interference for a user in cell 1, 2, or 3 is from the other two cells. The interference from BSs at further locations can be considered as a low-power background noise. Hence, in a large cellular network the optimization can be performed separately for each 3-sector cluster.

The parameter settings are as follows. The regional division depends on the BSs' on-off states. Specifically, if only one BS is active, as shown in Fig. 6(b), the cluster is divided into $M = 2$

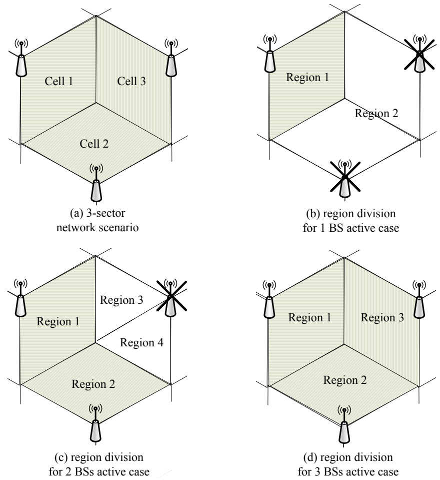

Fig. 6. Sectorized Multi-cell Erlang's approximation settings.

regions. The first region is the original coverage area of the active BS, and the second is that of the others. If two BSs are active (Fig. 6(c)), $M = 4$. The coverage area of the sleep BS is divided into 2 regions, which are served by the two active BSs, respectively. Finally, if all BSs are active (Fig. 6(d)), $M = 3$, and each region is covered by its own BS. The service rate is assumed to be the same in all cells $\mu_K = 1\text{s}^{-1}$. The traffic in the studied area follows the profile illustrated in Fig. 3. Assume that the arrival rate in sector b in time period t is $\lambda_t^{(b)} = \psi^{(b)}\lambda_t$, where $0 \leq \psi^{(b)} \leq 1, \sum_b \psi^{(b)} = 1$. We run the simulations for two setups: an asymmetric traffic distribution $\psi^{(1)} : \psi^{(2)} : \psi^{(3)} = 1 : 2 : 3$ and a symmetric distribution $\psi^{(1)} : \psi^{(2)} : \psi^{(3)} = 1 : 1 : 1$. The renewable energy profiles of three BSs are assumed identical as in reality, the renewable energy (ex. solar power) intensity will be almost equal in a cluster-sized region. The same energy profile depicted in Fig. 3 is adopted for all the BSs. For the proposed two-stage DP algorithm, we adopt greedy initial state settings discussed before.

Fig. 7 depicts the tradeoff curves of different algorithms for the symmetric traffic distribution case. Notice that the *BS on-off* algorithm only optimizes the BS on-off state assuming all subcarriers are active ($n_t^{(b)} = N$) so there is no opportunistic sleep ($\varphi_t^{(b)} = 0$). It is actually

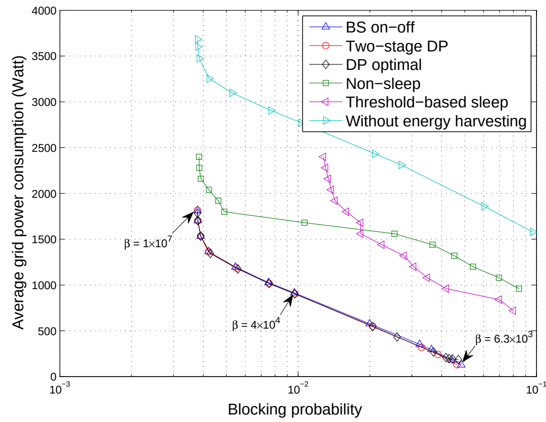

Fig. 7. Tradeoff curves between outage probability and grid energy consumption for 3-sector case. $K = 1, \psi^{(1)} : \psi^{(2)} : \psi^{(3)} = 1 : 1 : 1$. The renewable energy profile as in Fig. 3 is the same for three BSs. Some values of β are depicted correspondingly.

the first stage optimization in the two-stage algorithm. Also notice that for the heuristic non-sleep and threshold-based sleep algorithms, the joint traffic-energy aware adaptation algorithm is used in the second stage as it is better than the other heuristic algorithms. In the threshold-based sleep algorithm, we set two thresholds $\theta_1 < \theta_2$. If $\lambda_t \leq \theta_1$, only the BS with the heaviest traffic load is active. If $\theta_1 < \lambda_t < \theta_2$, the only BS with the lightest load sleeps. Otherwise, all the BSs are active. In this figure, we set $\lambda_{\max} = 7.5, \theta_1 = 3, \theta_2 = 6$. It can be seen that the two-stage DP algorithm performs the same as the optimal DP one, and the optimal solution is achieved only by adjusting BS sleeping policy, which is consistent with our analysis. The threshold-based heuristic sleep algorithm performs better than the non-sleep algorithm when the grid power is less than 1550Watt. In addition, the figure shows that using harvested energy can greatly reduce the power usage from grid (i.e. without energy harvesting).

The tradeoff between blocking probability and grid energy consumption under an asymmetric traffic distribution for a single user class ($K = 1$) is shown in Fig. 8. Unlike the symmetric traffic case, the proposed two-stage DP algorithm performs close to the optimal DP algorithm, and is better than the BS on-off algorithm. Hence, in addition to the BS on-off states, the adaptation

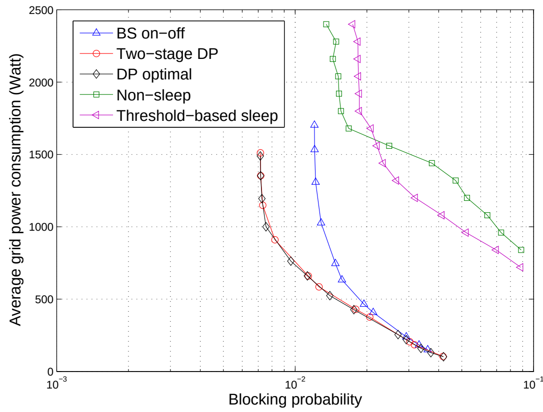

Fig. 8. Tradeoff curves between outage probability and grid energy consumption for 3-sector case. $K = 1, R_1 = 2\text{Mbps}, \psi^{(1)} : \psi^{(2)} : \psi^{(3)} = 1 : 2 : 3$. The renewable energy profile as in Fig. 3 is the same for three BSs.

of number of active subcarriers and opportunistic sleep ratio further improves the performance. It can be explained as follows. Reducing the number of active subcarriers reduces the available wireless radio resources (enhancing its own blocking probability) on the one hand, but on the other hand reduces the interference to the neighbouring cells (reducing neighbor cells' blocking probability). In the asymmetric traffic distribution scenario, if the number of active subcarriers of a low traffic load BS is reduced, the effect of interference reduction outweighs that of radio resource reduction as the blocking probability is quite low. As a result, we can adapt the number of active subcarriers to approach the optimal bound. On the contrary, there is no improvement by reducing active subcarriers in the symmetric traffic distribution scenario.

We also simulate the multiple user class case. Figs. 9 and 10 illustrate the tradeoff curves with $K = 2$ user classes (rate requirements are $R_1 = 2\text{Mbps}$ $R_2 = 0.5\text{Mbps}$) for the symmetric and the asymmetric traffic distribution, respectively. We assume $\lambda_{\max} = 12, \theta_1 = 3, \theta_2 = 10$, and each user class occupies half of the traffic. It can be seen that the performance is similar with the $K = 1$ case for the symmetric traffic distribution, but is different for the asymmetric traffic distribution. In particular, when a low blocking probability is targeted, the two-stage DP

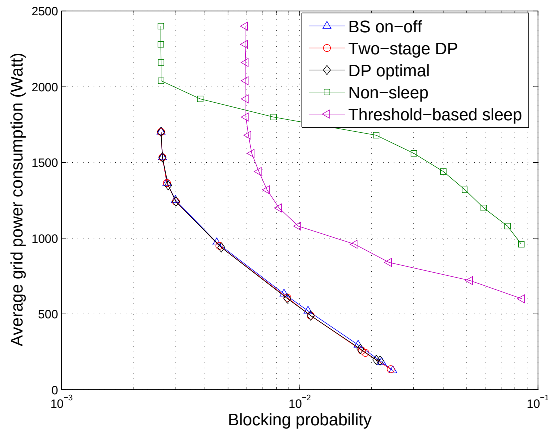

Fig. 9. Tradeoff curves between outage probability and grid energy consumption for 3-sector case. $K = 2, \psi^{(1)} : \psi^{(2)} : \psi^{(3)} = 1 : 1 : 1$. The renewable energy profile as in Fig. 3 is the same for three BSs.

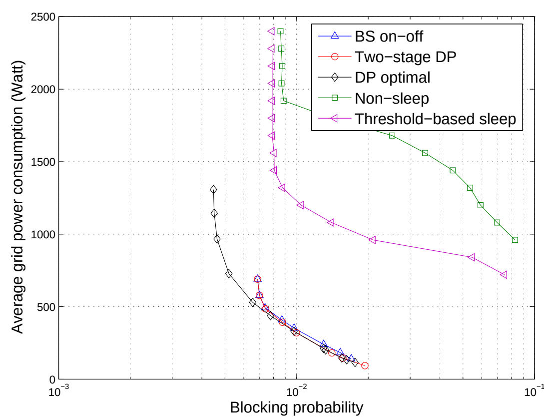

Fig. 10. Tradeoff curves between outage probability and grid energy consumption for 3-sector case. $K = 2, \psi^{(1)} : \psi^{(2)} : \psi^{(3)} = 1 : 2 : 3$. The renewable energy profile as in Fig. 3 is the same for three BSs.

algorithm is not close to the optimal solution any more. From the result, we find that no matter how large β is set, we can not activate all the three BSs by the BS on-off algorithm. The reason is that we assume all subcarriers are active in this algorithm, which causes very high interference when all the three BSs are active. However, the optimal DP algorithm can activate all three BSs

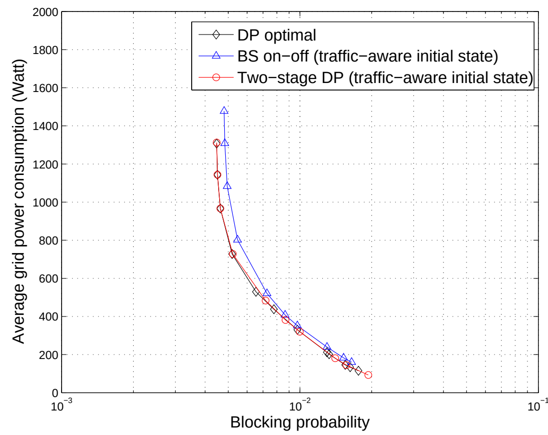

Fig. 11. Tradeoff curves between outage probability and grid energy consumption for 3-sector case with traffic-aware initial state. $K = 2, \psi^{(1)} : \psi^{(2)} : \psi^{(3)} = 1 : 2 : 3$. The renewable energy profile as in Fig. 3 is the same for three BSs.

by jointly optimizing the number of active subcarriers to reduce interference.

According to the above analysis, the performance gap between the proposed algorithm and the optimal policy is mainly due to the initial state of the first stage DP. We can improve the performance by carefully choosing the initial state proportional to the traffic condition, i.e., traffic-aware initial state settings. Specifically, when all the three BSs are active, we set $n_0^{(b)} = \lceil (a_1\psi^{(b)} + a_2)N \rceil$, where $a_1 = 1.2, a_2 = 0.4$, $\boldsymbol{\varphi}_0 = \mathbf{0}$, and rerun the algorithm. The result is shown in Fig. 11. We can see that the performance of the BS on-off algorithm is greatly improved, and the two-stage DP algorithm achieves the performance of the optimal DP. It further illustrates the importance of subcarrier adaptation for the asymmetric traffic case.

VI. Conclusion

This paper has studied the joint optimization problem of BS sleeping and resource allocation in a long-term point of view with the average network traffic profile and the harvested energy profile. The proposed two-stage DP algorithm is shown to achieve optimal performance in a symmetric traffic distribution scenario. In this case, we only need to determine BSs' on-off state and the active BSs activate all their subcarriers with sufficient power input. It further reduces the computational complexity. On the contrary, if the traffic is asymmetrically distributed, active subcarrier adaptation should be jointly optimized with BS sleeping to improve the performance. Numerical results show that for the asymmetric case with greedy initial state settings, if $K = 1, p_{\text{target}} = 1.25\%$, the two-stage DP algorithm reduces the grid power consumption by about 50% compared with the BS on-off algorithm. In this paper, we only consider the type of services with minimum rate requirement. Future work can study the energy management policies for the services which can tolerate some delay to exploit the energy-delay tradeoff. The other interesting research direction is to design frame-by-frame online policies to further improve the performance.

REFERENCES

[1] D. Valerdi, Q. Zhu, K. Exadaktylos, S. Xia, M. Arranz, R. Liu, and D. Xu, "Intelligent energy managed service for green base stations," *IEEE Globecom GreenComm. Workshop*, Dec. 2010

[2] J. Yang and S. Ulukus, "Optimal packet scheduling in an energy harvesting communication system," *IEEE Trans. Commun.*, Vol. 60, No. 1, Jan. 2012

[3] O. Ozel, K. Tutuncuoglu, J. Yang, S. Ulukus, and A. Yener, "Transmission with energy harvesting nodes in fading wireless channels: optimal policies," *IEEE J. Selected Areas Commun.*, Vol. 29, No. 8, Sept. 2011

[4] M. A. Antepli, E. Uysal-Biyikoglu, and H. Erkal, "Optimal Packet Scheduling on an Energy Harvesting Broadcast Link," *IEEE J. Selected Areas in Commun.*, vol. 29, no. 8, pp: 1712-1731, Sept. 2011

[5] J. Yang, O. Ozel, and S. Ulukus, "Broadcasting with an energy harvesting rechargeable transmitter, *IEEE Trans. Wireless Commun.*, Vol. 11, Issue 2, pp. 571-583, Feb. 2012

[6] J. Yang, S. Ulukus, "Optimal packet scheduling in a multiple access channel with energy harvesting transmitters," *IEEE J. Commun. Netw.*, Vol. 14, No. 2, Apr. 2012

[7] M. Gregori and M. Payar, "On the precoder design of a wireless energy harvesting node in linear vector Gaussian channels with arbitrary input distribution," *IEEE Trans. Commun.*, Vol. 61, No. 5, pp. 1868-1879, May 2013

[8] M. Gatzianas, L. Georgiadis, and L. Tassiulas, "Control of wireless networks with rechargeable batteries," *IEEE Trans. Commun.*, Vol. 9, No. 2, Feb. 2010

[9] D. P. Bertsekas, *Dynamic programming and optimal control*, 3rd ed., Athena Scientific, Belmont, Massachusetts, 2005

[10] D. Niyato, E. Hossain, and A. Fallahi, "Sleep and wakeup strategies in solar-powered wireless sensor/mesh networks: performance analysis and optimization," *IEEE Trans. Mobile Computing*, vol. 6, no. 2, Feb. 2007

[11] B. Medepally, N. B. Mehta, and C. R. Murthy, “Implications of energy profile and storage on energy harvesting sensor link performance,” *IEEE Globecom*, Nov. 2009

[12] S. Chen, P. Sinha, N. B. Shroff, and C. Joo,“Finite-horizon energy allocation and routing scheme in rechargeable sensor networks,” *IEEE Infocom*, pp. 2273-2281, Shang Hai, China, Apr. 2011

[13] N. Pappas, J. Jeon, A. Ephremides, and A. Traganitis, “Optimal utilization of a cognitive shared channel with a rechargeable primary source node,” *J. Commun. Netw.*, vol. 14, no. 2, Apr. 2012

[14] I. Krikidis, T. Charalambous, and J. S. Thompson, “Stability analysis and power optimization for energy harvesting cooperative networks,” *IEEE Signal Processing Letters*, vol. 19, no. 1, Jan. 2012

[15] B. T. Bacinoglu and E. Uysal-Biyikoglu, “Finite Horizon Online Lazy Scheduling with Energy Harvesting Transmitters over Fading Channels,” *IEEE ISIT*, Honolulu, HI, USA, Jun. 2014

[16] B. T. Bacinoglu and E. Uysal-Biyikoglu, ”Finite-horizon Online Transmission Scheduling on an Energy Harvesting Communication Link with a Discrete Set of Rates”, *Journal of Communications and Networks*, Vol. 16, No. 3, pp. 293-300, June 2014.

[17] D. Willkomm, S. Machiraju, J. Bolot, and A. Wolisz, “Primary user behavior in cellular networks and implications for dynamic spectrum access,” *IEEE Communications Magazine*, vol. 47, no. 3 pp: 88-95, 2009

[18] G. Auer, V. Giannini, I. Godor, P. Skillermark, M. Olsson, M. A. Imran, D. Sabella, M. Gonzales, C.Desset, and O. Blume, “Cellular energy efficiency evaluation framework,” *IEEE Vehicular Technology Conference (VTC Spring)*, 2011.

[19] M. Gorlatova, A. Wallwater, and G. Zussman, “Networking low-power energy harvesting devices: measurements and algorithms,” *Proc. IEEE Infocom*, 2011

[20] M. A. Marsan, G. Bucalo, A. D. Caro, M. Meo, Y. Zhang, “Towards zero grid electricity networking: powering BSs with renewable energy sources,” *10th Italian Networking Workshop*, Bormio, Italy, Jan. 9-11, 2013

[21] S. Zhou, J. Gong, Z. Yang, Z. Niu, and P. Yang, “Green mobile access network with dynamic base station energy saving,” ACM Mobicom, 2009

[22] E. Oh, K. Son, B. Krishnamachari, “Dynamic base station switching-on/off strategies for green cellular networks,” IEEE Trans. Wireless Commun., Vol. 12, No. 5, May 2013

[23] J. Gong, S. Zhou, and Z. Niu, “Optimal Power Allocation for Energy Harvesting and Power Grid Coexisting Wireless Communication Systems,” *IEEE Transactions on Communications*, vol. 61, No. 7, pp. 3040-3049, Jul. 2013

[24] Y. Cui, K. N. Lau, and Y. Wu, “Delay-aware BS discontinuous transmission control and user scheduling for energy harvesting downlink coordinated MIMO systems,” *IEEE Trans. Signal Processing*, Vol. 60, No. 7, Jul. 2012

[25] M. Zheng, P. Pawelczak, S. Stanczak, and H. Yu, “Planning of Cellular Networks Enhanced by Energy Harvesting,” *IEEE Communications Letters*, vol. 17, issue 6, pp. 1092-1095, Jun. 2013

[26] T. Han, N. Ansari, “On Optimizing Green Energy Utilization for Cellular Networks with Hybrid Energy Supplies,” *IEEE Trans. Wireless Commun.* vol. 12, no. 8, Aug. 2013

[27] J. Gong, S. Zhou, Z. Niu, and J. Thompson, "Energy-Aware Resource Allocation for Energy Harvesting Wireless Communication Systems," *IEEE Vehicular Technology Conference Spring*, Dresden, Germany, Jun. 2-5, 2013

[28] M. K. Karray, "Analytical evaluation of QoS in the downlink of OFDMA wireless cellular networks serving streaming and elastic traffic," *IEEE Trans. Wireless Commun.*, vol. 9, no. 5, May 2010

[29] S. Sesia, M. Baker, and I. Toufik, *LTE - the UMTS long term evolution: from theory to practice*, John Wiley & Sons, 2009

[30] R. Wang, J. S. Thompson, H. Haas, and P. M. Grant, "Sleep mode design for green base stations," *Communications, IET*, vol. 5, no. 18, pp. 2606-2616, Dec. 16, 2011

[31] B. Rengarajan, and G. de Veciana, "Architecture and abstractions for environment and traffic-aware system-level coordination of wireless networks," *IEEE/ACM Trans. Netw.* vol. 19, no. 3, Jun. 2011

[32] L. Kleinrock, *Queueing Systems*, vol. 1, John Wiley & Sons. 1976

[33] F. Kelly, *Reversibility and Stochastic Networks*, New York: Wiley, 1979.